Environ Earth Sci (2016) 75:911
DOI 10.1007/s12665-016-5730-2

ORIGINAL ARTICLE

Assessing geo-mechanical and leaching behavior of cement–silica-fume-stabilized heavy metal-contaminated clayey soil

Amir Reza Goodarzi[1] · **Mohammad Hossain Zandi**[1]

Received: 9 September 2015 / Accepted: 10 May 2016 / Published online: 19 May 2016

Abstract Although cement stabilization/solidification (S/S) is used extensively to remediate heavy metal (HM)-contaminated soils, it may show limited success in some applications. Hence, this study investigated the efficacy of silica fume (SF) as an industrial by-product in enhancing the performance of cement-based S/S. Artificially contaminated soils were first prepared by mixing kaolinite with zinc (Zn) at levels of 0–30 cmol/kg. Cement and cement/SF (CSF) mixture with 15 % cement replacement were used as S/S binders. The agents were separately added to the samples, and then, a set of tests were performed to assess the effectiveness of the treatments. The results show that the addition of sole cement markedly increases the HM retention capability of soil; however, this may be partly lost when the treated samples are acidified. The strength and compressibility potential of cement-treated specimens are also adversely affected by increasing Zn concentration. It appears that the incorporation of SF into the cement matrix reduces the destructive effects of aggressive environment and HM on the behavior of stabilized products. Additionally, based on the toxicity characteristic leaching procedure experiments, CSF blend is more efficient in immobilizing Zn with the lower dosage of binder and shorter curing time of samples compared to sole cement. These observations are mainly associated with both the extended synthesis of pozzolanic phases and maximized packing of particles upon CSF treatment, as is clearly confirmed by the XRD and SEM-EDX analyses. It is concluded that CSF content of 1 wt% per 1 cmol/kg of HM can successfully remediate the zinc-contaminated soils.

Keywords Zinc-contaminated soil · Stabilization/solidification · Silica fume · Geo-mechanical properties · Microstructure

Introduction

In recent years, with rapid industrialization and urbanization, soil contamination caused by heavy metal-bearing wastes has been a serious problem worldwide (Moon et al. 2010; Çoruh et al. 2013; Wang et al. 2015a). Heavy metals (HMs) not only are hazardous to public health because of their toxicity and bioaccumulation, but also can lead to the degradation of mechanical behavior of soils, which may pose considerable distress to civil structures (Kumpiene et al. 2008; Yong et al. 2009; Li et al. 2015). As such, it is necessary to implement cost-effective and versatile remediation technologies for the contaminated lands that pose the minimum threat to the environment and at the same time ensure that the engineering properties of treated materials are not adversely affected to reuse or reconstruct over them. Stabilization/solidification (S/S), which involves mixing a binding agent into the contaminated media, is a typical such operation which began in the early 1970s (Chen et al. 2009; John et al. 2011; Zhang et al. 2015). By and large, the S/S application for heavy metal-contaminated soils utilizing pozzolanic binder has proved as an effective and practical method (Coz et al. 2009; Kogbara et al. 2013; El-Eswed et al. 2015). The high strength, low permeability and relatively high durability of cement-based S/S products make cement the most adaptable stabilizing agent currently available for the

✉ Amir Reza Goodarzi
amir_r_goodarzi@yahoo.co.uk

[1] Faculty of Engineering, Hamedan Branch, Islamic Azad University, Hamedan, Iran

immobilization of HMs in soils. However, previous studies have indicated that cement may show limited efficiency in some applications (Malviya and Chaudhary 2006; Tantawy et al. 2012; Du et al. 2014a). Such disadvantages and the increased environmental costs associated with the production of cement are leading researchers to develop alternative agents or additives (e.g., fly ash), especially those that are more effective and less costly, to remedy contaminated soils (Voglar and Lestan 2013; Xi et al. 2014; Wang et al. 2015b). Silica fume (SF) is a by-product material produced in large amounts throughout the world from the manufacture of silicon or ferrosilicon alloys. The proper disposal of SF as an industrial waste is one of the major issues for environmentalists since leaving it directly in the environment may cause severe health problems (Li et al. 2014). On the other hand, the amorphous structure, high SiO_2 content (more than 85 %) and large specific surface area (about 20 m^2/g), make the SF reactive to the alkali product of cement to produce the calcium silicate hydrate (CSH) phase, which is expected to show advantages in terms of mechanical capacity and durability of S/S products (Jun et al. 2001; Li et al. 2014). Additionally, silica fume, as an additive, can partially be replaced with cement, thus contributing to waste recycling and also reducing the production demand for cement that can mitigate carbon emissions, since it has been reported that the production of one ton of cement, on average, generates 0.7–1 tons of carbon dioxide (Tsai et al. 2014). Based on a review of current literature (Chauhan and Kumar 2013; Elaty and Ghazy 2014; Fernández-Carrasco et al. 2014; Benaicha et al. 2015; Hot et al. 2015; Kang et al. 2015; Maheswaran et al. 2016; Zhang et al. 2016), the beneficial influence of silica fume on the properties of cement composite can be generally analyzed from chemical and physical aspects. Chemical effects involve the secondary reaction between amorphous silicon dioxide (SiO_2) of SF with free calcium hydroxide as a weak part of the cement hydration product, which forms additional amounts of CSH linkages. This can enhance the bonding of solid phase and improve the density of binary system with SF and cement, promoting the compressive strength development significantly (Wei et al. 2012; Koksal et al. 2015). Physical effects are embodied in the filling impact. Because silica-fume particles of SF are 100–150 times smaller than cement particles and because such particles have near-perfect spheres, they occupy the voids created by free water in the matrix and provide a much denser pore microstructure, which in turn may cause a reduction in capillarity and can block micro-channels, thereby exhibiting good fixation efficiency of HMs and offering resistance to the flow of liquids or gases (Li et al. 2014). This will result in the decrease in the permeability of the binary system and can also increase the resistance of aggressive environment (Saraya 2014; Liu et al. 2015; Koteng and Chen 2015). Apart from pozzolanic activity of SF and its filling effect, silica fume affects the hydration kinetics. As silica-fume particles provide more nucleation sites, they accelerate the hydration reactions of cement during the early stages, a process that contributes toward a decrease in the setting times (Abo-El-Enein et al. 2015; Muller et al. 2015; Maheswaran et al. 2016). Also, the SF can improve the interface bond strength between hardened paste and aggregate. This is mainly attributed to the fact that the crystalline orientation degree, the crystalline size and the content of calcium hydroxide at the interface are dramatically decreased when silica fume is added to the cement, thus making the interfacial transition zone (ITZ) of aggregates and binding paste matrix denser (Jalal et al. 2015; Zhang et al. 2016). In other words, besides modifying the ITZ, the chemical effects of SF transform the harmful $Ca(OH)_2$ to secondary CSH gel which fills in the gaps between hydration product of cement and will significantly reduce both the interfacial region's porosity and the deposition of a portlandite rim, which lead to improved strength performance and durability of the composite cementing system (Liu et al. 2015; Nili and Ehsani 2015). On the whole, the positive effects of the mechanical and physical properties that SF as a pozzolanic material confers on concrete, problematic soils, HMs-bearing foundry sludge and municipal solid waste incineration (MSWI) fly ash have been previously investigated in several research (Kalkan 2011, 2013; Nazari and Riahi 2011; Li et al. 2014; Hot et al. 2015; Sanjuán et al. 2015; Zhang et al. 2016); however, there is a lack of detailed studies on different aspects of the cement-SF (CSF) blend for treatment of contaminated soils. Thus, the present research was conducted to address the efficacy of CSF in enhancing the geomechanical characteristics of S/S soil with different levels of zinc, as evidenced by a set of macro- and micro-level tests. This achieves the objectives of (1) reducing the restrictions associated with the cement S/S products in the presence of HMs, (2) providing reliable data for recycling SF without having to be deposited in a landfill site and (3) decreasing the cement consumption and therefore, mitigating carbon emissions.

Materials and methods

Materials

Kaolinite has a relatively low surface charge and a limited surface activity. It also has a more stable structure and no significant shrink-swell capacity in comparison with the other clay minerals such as montmorillonite (Chemeda et al. 2015). Thus, in this study, kaolinite identified as "super zenous kaolinite" from northwest Iran was used to

Table 1 Engineering and geo-environmental properties of kaolinite sample

Characteristics	Quantity measured
Mineral composition in decreasing amount	Kaolinite (≈70 %), quartz
pH	8.82
EC (mS/cm)	0.15
SSA (m^2/g)	25
CEC (cmol/kg)	11.2
Clay fraction (%)	68
Specific gravity (G_S)	2.69
Liquid limit (LL) (%)	38.2
Plasticity index (PI) (%)	19
Soil classification	CL
Maximum dry density (gr/cm^3)	1.56
Optimum moisture content (%)	28.5
Unconfined compression strength[a] (MPa)	0.18

[a] The soil sample was mixed with the optimum moisture content and compacted at the maximum dry density

prepare artificially contaminated soil. To characterize the soil sample, the engineering properties were determined according to ASTM methods (ASTM 2006). The soil geo-environmental analyses were also conducted using the procedures described in the manual of the EPA (1983). The electrical conductivity (EC) and pH of the soil sample were measured in 1:10 soil suspension. These properties of the soil sample are given in Table 1. In this table, the optimum moisture content (28.5 %) was determined by means of the standard Proctor compaction test, which is designated by ASTM D698 (ASTM 2006). The agents for S/S were sole cement and a mixture of cement and silica fume with 15 % cement replacement. The cement was replaced with 15 % silica fume because higher percentage of replacement might have occupied the pore spaces and could have limited the extent of cement hydration reactions (Asavapisit et al. 2001; Jun et al. 2001). The chemical compositions of the used cement and SF were determined by the XRF analysis (see Table 2), which indicated that the SF used had a noticeable amount of SiO_2.

Unlike Cr, As, Hg and Cd, zinc is an essential moderate element for organisms and plant growth, and also under acidic conditions, it is one of the most soluble and mobile of the divalent trace metal cations because of which the concentration of zinc in natural soil is usually higher than other heavy metals (Ko et al. 2007; Stephan et al. 2008; Erdem and Özverdi 2011). Moreover, Zn represents one of the most common HMs found in the contaminated soils (Coz et al. 2009; Voglar and Leštan 2010; Li et al. 2014; Soares et al. 2015; Chiang et al. 2016) and it is listed as a priority pollutant by the EPA (Moon et al. 2010; Saeed et al. 2015). The anthropogenic source of zinc pollution is mainly the emission

Table 2 Chemical compositions of used cement and silica fume

Chemical composition	Percentage in weight (%)	
	Cement	SF
SiO_2	21.52	90.6
Al_2O_3	4.95	1.47
Fe_2O_3	3.82	1.93
CaO	63.49	1.52
MgO	1.55	0.42
Na_2O	0.48	0.63
K_2O	0.75	1.31
P_2O_5	<0.1	0.28
SO_3	2.13	0.41
TiO_2	<0.1	<0.1
Loss of ignition	1.11	1.33

of nonferrous metals from smelters. Another significant source of zinc in contaminated soils is the burning of coal and waste, municipal sewage, the metallurgical industry and tire wear from cars (Malamis and Katsou 2013; Dmuchowski et al. 2014; Shen et al. 2016). Besides, Zn has widely been used in preparing artificially heavy metal-contaminated soil samples in previous works (Ouhadi et al. 2006, 2010; Zhou et al. 2009, Wei et al. 2012; Du et al. 2013, 2016). Therefore, in line with the aims of the present study, zinc nitrate ($Zn(NO_3)_2 \cdot 6H_2O$) was used as the source of heavy metal to prepare the artificially HM-contaminated soil samples. The source chemical of zinc was selected in the form of nitrate because it is inert for the cement hydration reactions (Cuisinier et al. 2011). Also, the clayey soils with nitrate anions undergo less change in their hydromechanical parameters as compared to the other types of anions such as carbonate (Goodarzi and Akbari 2014). On the other hand, based on the previous studies (Chen et al. 2009; Yan et al. 2013; Du et al. 2014b), the combined pollution of heavy metals can affect the soil behavior and the S/S process. Thus, in order to avoid the complexity of the chemical reactions and to better interpret the effects of SF on the cement performance, only one type of pollutant (i.e., zinc) was used. It should be noted that the levels of zinc concentration used to prepare artificially contaminated soil samples were set as 0–30 cmol kg^{-1} (0 to ≈2 %). Such concentrations are sometimes encountered at waste disposal sites and contaminated lands of urban areas as reported by Du et al. (2014a). The cement and CSF blend dosages were set at a range of 5–30 % by total weight of the solids in the oven-dry state.

Samples preparation and experimental methods

To investigate the chemical interaction between HM and the clay lamellae system, with and without agents, a series of batch equilibrium tests were performed according to the EPA (1983). For this purpose, the soil–electrolyte

suspensions were prepared at a 1:20 soil to solution ratio by adding different concentrations of zinc nitrate. The suspensions were equilibrated (shaken for 24 h) and then were centrifuged at 3000 rpm for about 10 min. The amount of Zn in the supernatant was analyzed using an atomic absorption spectrophotometer modeled GBC-Xplor AA. The pH and zeta potential of the soil–solutions were also recorded. The experimental values of the zeta potential (ζ) can be obtained from electrokinetic tests such as electrophoresis and electroosmosis and from measurements of the streaming potential and sedimentation potential (Kaya and Fang 2000; Kaya and Yukselen 2005). The electrophoresis and electroacoustics are mainly designed for more stable suspensions of small (<10 μm) particles; however, for measuring ζ of larger particles which do not form stable suspensions (such as the condition of samples in this study), the streaming potential and/or sedimentation potential can be used (Hunter 2013; Goodarzi et al. 2016). Herein, ζ of the soil–electrolyte suspensions was determined using an automated streaming potential instrument (a zeta meter modeled Microtrac ZETA-check). As in many previous studies (Kogbara et al. 2013; Wang et al. 2015a), the unconfined compression strength (UCS) test was used to evaluate the efficiency of stabilizers on the mechanical properties of S/S materials. For performing the UCS tests, the pre-weighed dry soil required for the maximum dry density was mixed with 30 % laboratory Zn-contaminated water. To get the desired concentration, the zinc nitrate was weighed and dissolved in distilled water and then added to the soil sample. The pre-weighed S/S agent was added to the contaminated soil and was thoroughly mixed for a period of 10 min in a mechanical mixer. Then using a hydraulic jack, the homogenized mixtures were statically placed inside cylindrical steel molds, 35 mm in diameter and 70 mm in length, to achieve the maximum dry density. After the extrusion of specimens from the mold, they were placed in airtight plastic bags and were cured in a warm humid chamber at temperature 22 ± 1 °C and with a relative humidity of 85 %. At the end of each curing period (i.e., 1, 7 and 28 days), the UCS tests were performed on the samples following ASTM D-2166. To determine the compression behavior of treated contaminated soil, the homogenized specimens were mixed in a way similar to that used for the UCS test and were confined in the oedometer ring, 50 mm in diameter and 20 mm in height. After adequate curing, the consolidation tests were conducted according to ASTM D-2435, for measuring settlement potential of the samples which were initially loaded with a pressure of 25 kPa that gradually increased by an increment ratio of 1 to a maximum pressure of 800 kPa. The duration of each loading was 24 h.

The leaching of HM from the natural and S/S kaolinite samples into the solution was assessed by the toxicity characteristic leaching procedure (TCLP) as defined by the EPA method 1311. For this purpose, the samples similar to that used for the UCS test were first prepared and then were crushed to reduce their particle size to less than 2.0 mm. After this, they were agitated in the extraction fluid at a liquid to solid ratio of 1:20 for 18 h at 30 rpm. Because the pH values of all specimens were mainly greater than 5, the extraction fluid with a pH of 2.88 ± 0.05 was used for all the TCLP tests (Choi et al. 2009; Moon et al. 2010; Zha et al. 2013). After the extraction, the final pH of the leachate was measured and then filtered through a 0.45-μm membrane filter to remove suspended solids. It was then stored in the cold for the determination of HM concentration, using the AA apparatus. It is worth mentioning that all macro-level tests were done in triplicate and the average values were reported to verify the reproducibility of data. However, due to precision in preparing and testing the samples, very little difference was observed between the results of repeated measures of each test. To further evaluate the mechanisms involved in the S/S process, the microstructure of samples was monitored using the scanning electron microscope (SEM) and X-ray diffraction (XRD) powder tests. Air-dried pieces of the soil samples collected from posttest UCS specimens were used for the microanalyses. Images of samples were magnified 3000 times by means of a SEM modeled VEGA3 TESCAN. Energy-dispersive X-ray (EDX) tests were also used during SEM testing to quantitatively measure the composition of small-surface regions. For XRD tests, the samples were first grinded to produce fine homogeneous powders. Each sample was then placed into an elliptical opening of an aluminum holder and evenly distributed along the microscope slide until a smooth surface was obtained. Finally, they were scanned in the 2θ range of 2–60° for their XRD spectra using a Bruker D8 apparatus with Cu-Kα radiation.

It should be noted that the reason to use artificial contaminated kaolinite soil samples in this study was to ensure that the mineralogy compositions, pore fluid chemistry, type of exchangeable cations and pollutants characteristics of samples in all of the tests were similar because these parameters are very effective in the S/S process and in the case of using natural soils they may be different, which can affect the reactions between soil and stabilizer. Therefore, to avoid confusion in interpreting the results, due to the differences in the properties of samples, and also to allow a better comparison of the test results, especially in the microstructure experiments, the artificial contaminated soil samples with similar mineralogy, exchangeable cations and type of pollutant were prepared at the laboratory-controlled condition. Moreover, kaolinite has a relatively low surface charge and a limited surface activity. Also, it has a more stable structure and no significant shrink-swell capacity that may be effective in the S/S process. Thus, in line with

previous works (Ouhadi et al. 2010; John et al. 2011; Du et al. 2013), artificial contaminated clayey soil samples were prepared with kaolinite due to its relatively well-defined physical and chemical properties to allow better understanding of key interactions.

Results and discussion

Batch equilibrium test results of Zn-spiked soil slurries

Figure 1 compares the adsorption of zinc ions to the soil samples with different dosages of cement. As indicated in this figure, the maximum adsorption of Zn to the natural kaolinite (without agent) was approximately 18 cmol kg^{-1} (i.e., $\approx$1 %) which was lower than the quantity of zinc ($\approx$2 %) that may be typically found in the contaminated lands of urban areas. The results also showed that an increase in the HM levels decreased the retention capacity of kaolinite soil sample, similar to that in the montmorillonite clays described by Ouhadi et al. (2006). For instance, at 10 cmol kg^{-1} zinc concentration, all the Zn ions were approximately retained by the clay–electrolyte system and the soil HM retention was 96 %; however, it reached to about 61 % following the further increase in the Zn contaminant up to 30 cmol kg^{-1}. On the other hand, the addition of cement had a major effect on the soil adsorption and the Zn level in the supernatant dramatically decreased proportionate with the increase in the cement dose. As Fig. 1 shows, the cement-treated kaolinite was able to completely retain Zn ions when enough amount of binder ($\approx$10 %) was added to the soil sample. This observed difference between the retention capability of natural and treated samples can be attributed to the immobilization of HM by various mechanisms (such as sorption, surface complexation, precipitation and micro- or macro-encapsulation) at the presence of cement (Chen et al. 2009; El-Eswed et al. 2015). In addition, since kaolinite has a pH-dependent charge, at low pH levels, which can arise from the hydrolysis of HM in the electrolyte system (see Eq. 1 below), the clay particles may have a lower negative charge, and thus a lower tendency to adsorb heavy metals (Ouhadi et al. 2006).

$$M^{2+}(aq.) + nH_2O \leftrightarrow M(OH)_2^{2-n} + nH^+ \quad (1)$$

In an attempt to further elucidate the effects of HM and cement on the retention properties of soil, the pH and zeta potential (ζ) values of soil samples were measured and presented in Figs. 2 and 3. According to the results presented in Fig. 2, the increase in the Zn concentrations considerably decreased the soil pH due to raising the

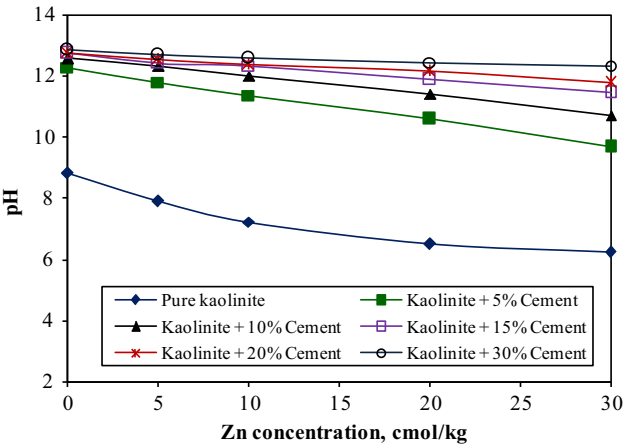

Fig. 2 pH variation of kaolinite sample versus the addition of cement and zinc contaminant

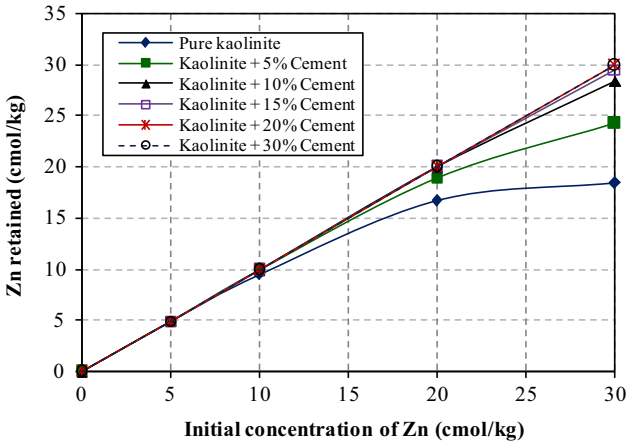

Fig. 1 Adsorption isotherm for the natural and cement-treated kaolinite sample

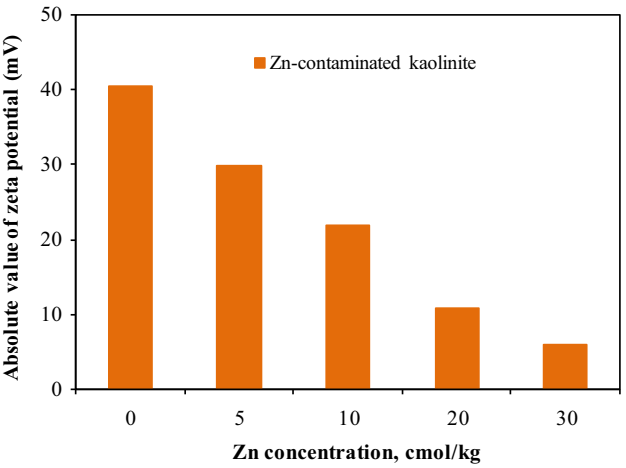

Fig. 3 Effect of Zn concentration on the zeta potential values of untreated kaolinite sample

hydrogen ions (H^+) in pore fluid as a result of the hydrolysis phenomenon. This is because in this case, the surface charge density of the clay particles will be made less negative (Goodarzi and Akbari 2014) because of the decrease in the surface concentration of hydroxyl ions (OH^-), which contributes to a reduction in the soil retention capability, as shown in Fig. 1. This process was confirmed by the observed reduction in the absolute value of the ζ upon increasing the HM concentrations (Fig. 3) which indicated a lack of electrical charges on the contaminated clay particles (Kaya and Fang 2005; Goodarzi et al. 2016), and hence, a lower HM retention occurred. Figure 2 clearly shows that the addition of cement caused a noticeable change on the extent and trend of pH variation in the soil samples. The pH values of uncontaminated kaolinite changed from an initial pH of 8.82–12.4 with 5 % cement and reached to about 13 with the further addition of agent. The increase in pH level was a result of dissolution of $Ca(OH)_2$ produced in large quantities during the hydration reactions of cement, providing an increase in the buffering capacity of the S/S materials (Kogbara et al. 2013). Therefore, the slope of the pH-Zn-added curve decreased as the cement dosage increased. This signifies that there was less impact of heavy metal on soil pH due to the decrease in the hydrolysis phenomenon as a result of increase in the heavy metal adsorption in the presence of cement, a finding highly consistent with the results in Fig. 1.

Leachability of Zn from cement and CSF-treated soils

While the batch test results indicate that the addition of cement significantly increases the HM retention capacity of the contaminated soil, this also needs to be characterized using reliable leaching tests such as TCLP, which can be closely linked to a suitable long-term site management strategy (Çoruh et al. 2013; Zhang et al. 2015). Therefore, the mobility of HM from the S/S products was determined by the standard TCLP extraction procedures as described in the materials and methods. The results of Zn toxicity leaching test and final leachate pH for the cement and CSF-treated samples after 7 and 28 days are summarized in Fig. 4. It can be seen that the leached Zn from the untreated kaolinite samples generally exceeded the Zn legislative concentration limit of 5 mg/L specified by the other studies (Ruiz and Irabien 2004; Voglar and Lestan 2013), emphasizing the need for remediation. On the other hand, the treated soils exhibited lower amounts of leached Zn that decreased with the rising binder dosage and time of curing. This can be attributed to an increased formation of cement hydration products which can strongly raise the potential for chemical immobilization of HM in the S/S products (Du et al. 2014a). The results in Fig. 4-a reveal that although the leaching of zinc dramatically decreased with an increased cement content, the addition of binder even up to 30 % and following 28 days of curing could not meet the full needs of HM immobilization in the heavily zinc ($\approx$2 %)-contaminated samples, and thus, a higher amount of the agent should be added to satisfy the Zn permissible limit. This is unlikely to occur in the batch equilibrium test results. For example, the immobilized proportions of HM from the solidified samples with 30 cmol/kg Zn and 15 % of cement in TCLP extracts decrease by nearly 11 % as compared with the included results in Fig. 1. In fact, the presence of Zn can be expected to hinder or decrease the formation of cementing compounds (Qiao et al. 2007; Moon et al. 2010; Wang et al. 2015b), which plays a key role in controlling leaching of pollutants from the S/S products, and therefore, the TCLP tests exhibited a higher Zn mobility as compared to the batch equilibrium tests. Besides, the compression of the pH values in Figs. 2 and 4a indicates that the experiments performed in the acidic conditions of TCLP can break the pH balance of the treated samples, causing degradation of cementitious structure and resolubilization of heavy metals (Kogbara et al. 2013), thus resulting in a large number of Zn ions which leach out during the TCLP tests compared with the batch tests.

As the results in Fig. 4b show, the addition of cement/silica-fume mixture had an obvious positive effect on zinc immobilization compared with sole cement. The pH values upon such treatment are slightly lower relative to the cement-treated samples. These observations can be explained by the higher pozzolanic activity of CSF blend, as would be evaluated by the XRD and EDX tests. In fact, calcium hydroxide, a cement hydration product, can be partly consumed by silica fume during the pozzolanic reactions (Asavapisit et al. 2001; Kalkan 2011), and hence, the presence of lower unreacted $Ca(OH)_2$ in the samples with CSF blend decreased the pH of the system. On the other hand, the development of secondary calcium silicate hydrates with the introduction of SF to cement produces more cementitious compounds which may strongly bind the soil particles together and incorporate more HM in siliceous solids (Coz et al. 2009). This encapsulation protects Zn from further attack by the TCLP solution, causing a decrease in the HM leachability. In addition, the extreme fineness of SF particles (the near-perfect spheres with diameters ranging from 20 to 500 nm) could make them very efficient fillers that result in a reduced volume of larger soil pores and probably serve to distribute the new crystalline phases in a more homogenous fashion in the available space, i.e., the formation of denser microstructure (see SEM images), which exhibit good fixation efficiency of HMs (Jun et al. 2001; Li et al. 2014). Therefore, the leaching of Zn ions upon CSF treatment was lower than

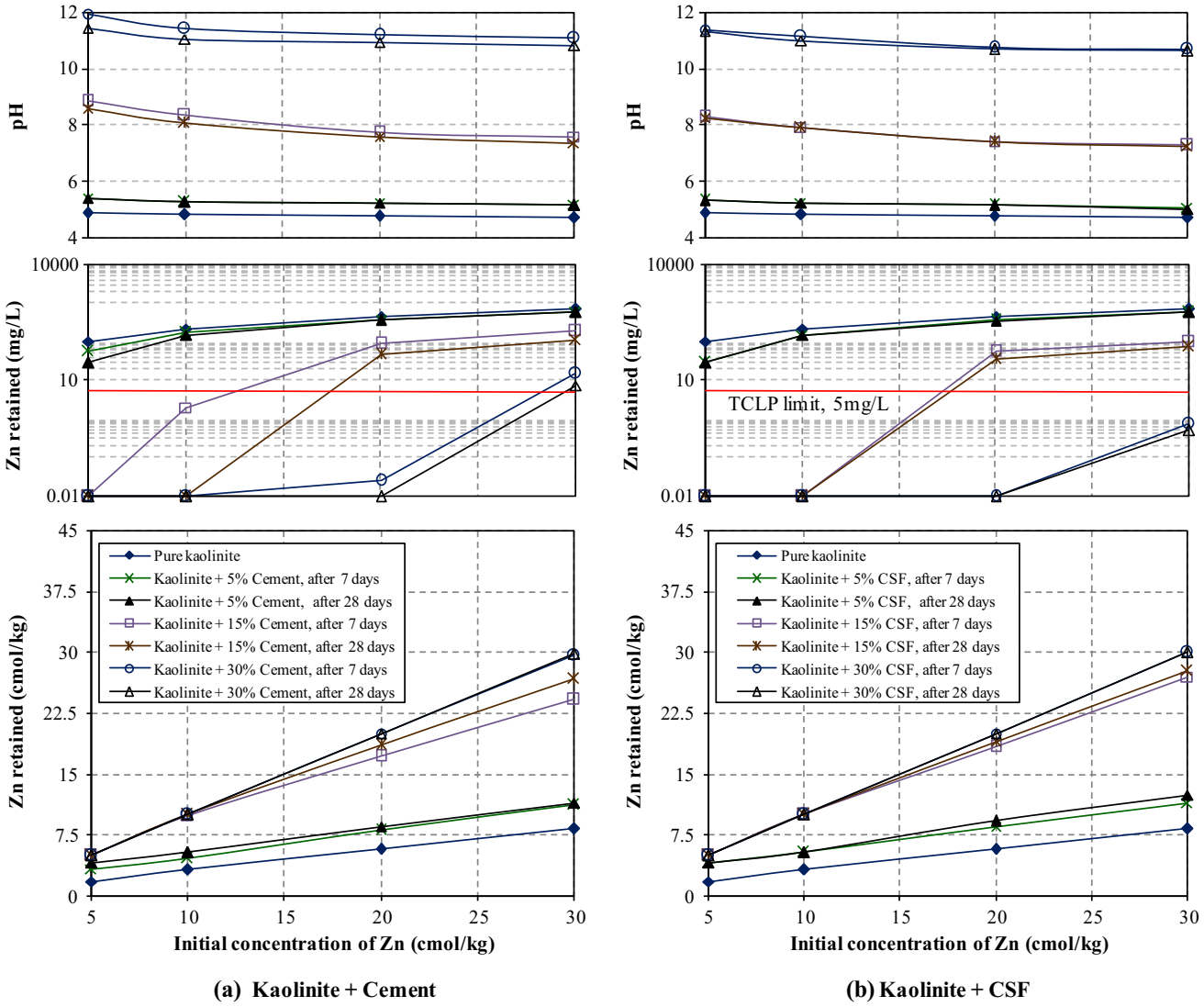

Fig. 4 TCLP Zn retained along with TCLP pH of samples upon cement and cement/silica fume (CSF) treatment after 7 and 28 days of curing

that of those in the presence of sole cement. This finding supports the beneficial effect of SF on the increase in resistance of treated soil to aggressive environments with the lower dosage of binder and shorter time of curing. Indeed, as illustrated in Fig. 4, the addition of 30 % CSF to the heavily zinc-contaminated soils could satisfy the standard limit of 5 mg/L following 7 days of curing and could reduce the Zn release by as much as 99.9 %. However, adding cement even up to 30 % and following 28 days of curing could not meet the full needs of HM immobilization in the samples. Another notable observation from the TCLP experiments was that the Zn leachability of the S/S products (with cement or CSF agent) obviously decreased in the high pH zone ($\approx$11), indicating that solution pH is an important factor for HM immobilization, as stated by other authors (Xi et al. 2014; Zhang et al. 2015). Moreover, one can conclude that the mentioned microstructural reorganization at the presence of CSF blend may also improve the engineering properties of S/S products, as will be experimentally evaluated by the macro-level tests in this research.

Geo-mechanical properties of cement and CSF-treated soils

The unconfined compressive strength (UCS) test has been widely used to monitor the progress of hydration reactions and to evaluate the effectiveness of S/S process (Hekal et al. 2011). Generally, the required mechanical strength for a treated material should be evaluated on the basis of the applied loads. For example, an UCS of 0.35 MPa is accepted by the US EPA to be suitable for physical

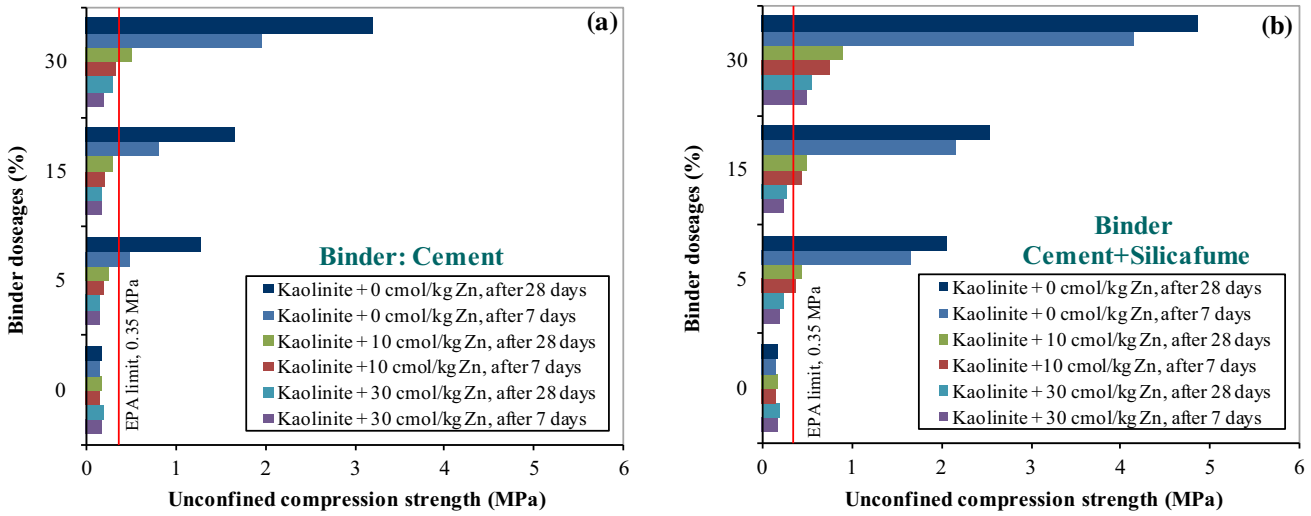

Fig. 5 Effect of Zn concentration, curing time and stabilizer content on the unconfined compressive strength of both cement and CSF-treated samples

integrity of the stabilized waste to stand typical overburden pressures in a landfill disposal (Voglar and Lestan 2013). Figure 5 shows the influence of agents and curing time on the UCS variation of natural and Zn-spiked kaolinite samples. As it can be seen, the uncontaminated soil exhibited the trend of UCS development in response to addition of binder. This is mainly due to increase in the cementitious compounds that leads to particles interlocking, and therefore, a significant strength gain (Goodarzi and Salimi 2015). Following the increase in curing time, a higher level of strength was also achieved which is ascribed to the fact that the strength of cement-treated clays is expected to increase with time as long as alkaline environment is present because the development of cement hydration and the completion of the secondary reaction (i.e., pozzolanic activity) can last for months after mixing (Lemaire et al. 2013). On the other hand, Fig. 5a shows that the UCS of cement-treated samples clearly dropped as the HM levels increased in line with the findings of Tantawy et al. (2012) and Saeed et al. (2015). Such an observation can be a result of the decrease in the pH levels following the increase in HM concentration (see Fig. 2). This is because the cementitious products are mainly unstable at pH < 10.8, and hence, the S/S performance would be diminished with the reduction in pH (Du et al. 2014a). Another explanation is that the presence of Zn ions may retard the cement hydration reactions due to the generation of a series of detrimental compounds, such as calcium zincate (Chen et al. 2009; Moon et al. 2010), as was clearly confirmed by the micro-level tests. These new products can coat cement particles and form a barrier separating them from water (Wang et al. 2015b), and therefore, hinder or decrease the cementitious minerals formation, resulting in the strength reduction in S/S products.

In terms of quality acceptance, considering the EPA criterion (UCS > 0.35 MPa), the presented results in Fig. 5a indicated that with the addition of cement even up to 30 %, sufficient strength values were observed only for the Zn levels approximately lower than 10 cmol kg^{-1}. It can be inferred that the specimens with the higher Zn contents may be successfully treated changing the composition of the agent (i.e., increasing the cement dosage or using additive). Figure 5-b displays the strength properties obtained upon CSF treatment after 7 and 28 days of curing. According to the results presented in this figure, although a further increase in zinc concentration promoted a decrease in the UCS values, Zn-spiked soil/CSF mixtures showed higher strength than the cement-treated samples did. It means that the deleterious effect of HM on the mechanical capacity of stabilized soils would be decreased in the presence of CSF blend, and there would be relatively higher strength (up to 50 %) compared with sole cement, indicating a better performance of CSF just as was the case for the TCLP tests. This behavior is mainly due to the excessive and rapid consumption of $Ca(OH)_2$ which is quickly formed during the hydration of cement as a result of high reactivity of SiO_2 in silica fume (Nazari and Riahi 2011). Therefore, the cement hydration and pozzolanic reaction are accelerated and augmented, giving additional calcium silicate hydrate which eventually increased the mechanical capacity of stabilized materials. This is because the CSH gel formation is one of the primary contributors of the development of cementation bonding and the strength enhancement of S/S products (Qiao et al. 2007; John et al. 2011). Those excess pozzolanic activities and production

of secondary CSH gel, as clearly identified by the micro-level tests (see Figs. 9, 11), can also occupy the soil void space and thereby can contribute to a better fixation of zinc ions, as shown by the TCLP experiments in the present study. Based on the UCS test results, it can be seen that the CSF content of 30 % upon 7 days of curing would be a conservative choice for the S/S of heavily Zn-spiked specimens ($\approx$with 30 cmol/kg zinc) to satisfy the requirements of EPA-accepted criterion of the UCS value (>0.35 MPa).

While in many other studies (Choi et al. 2009; Tantawy et al. 2012; Kogbara et al. 2013; Saeed et al. 2015) the efficiency of agents on the geo-mechanical properties of S/S materials has been assessed by the UCS values, very little attention has been given to the compression behavior of stabilized contaminated soil, which is important for the deformation analysis, and safe design of new civil structures being proposed at the remediated site (Ouhadi et al. 2014; Du et al. 2014b). Thus, to take into consideration the impact of interactions between the binders and HM on soil settlement, a series of consolidation experiments were performed on the clean and contaminated samples. The compression index (C_C), which is an indication of compressibility, was also measured by means of the $e-\log\sigma'_v$ compression curves. Figure 6 presents the variation of this coefficient for soils with different percentages of amendments cured over 28 days. As a representative, the results of compression stages in terms of final void ratios for soil samples at agent dose of 30 % are also shown in Fig. 6. It is evident from this figure that the compression behavior of the S/S products was greatly influenced by both the agent characteristics and HM concentration. It is not uncommon to see that there is a significant decrease in the C_C values of stabilized uncontaminated soils with an increase in the percentage of binder, which points to their tendency to resist the external load (Lemaire et al. 2013; Ouhadi et al. 2014), as shown by the UCS tests. On the other hand, the results in Fig. 6 indicate that at each specific applied loading, the contaminated soil samples reflected a higher settlement and the C_C tended to rise rapidly as the Zn concentration increased. It means that the presence of zinc resulted in a destructive influence on the prevention or reduction in treated soil compressibility which could be due to the degradation of cementation bonding that would reduce the soil resistance to overburden pressure. This interpretation is supported by the XRD data that show the decrease in the formation of cementing compounds under the application of HM. However, this deteriorating impact would be reduced in the case of CSF blend and consequently there was less increase in the C_C values after the interaction of stabilized samples with zinc ions. A possible explanation for this finding which is in line with the TCLP and UCS test results could be a consequence of the lower porosity and stiffer performance the samples reached upon the CSF treatment resulting from the densification of microstructure (see SEM images) either by the filler effect of silica fume or by the greater development of cementation bonding due to increasing the quantity of CSH gel formation, as was previously addressed.

Besides the strength and compression assessments, permeability is a prominent factor in controlling leaching of pollutants into and from the treated materials; hence, it is an important parameter to evaluate the long-term performance of S/S process (Antemir et al. 2010; Kogbara et al. 2013). Therefore, the variation of permeability coefficient, k, of treated samples with different levels of the Zn under a vertical pressure of 200 kPa was calculated from the results of the oedometer tests and depicted in Fig. 7. As it can be seen, the soil permeability depends on the cement dosage and the Zn concentration. The k values continuously decreased as the agent content increased. This can be associated with the fact that permeability chiefly depends on the geometric arrangement of soil particles (Goodarzi and Akbari 2014). The growth of cementing compounds with increasing the additive content could generally fill the void spaces and could block off the micropores of soil, which result in the decrease in the soil permeability. On the other hand, the presence of Zn caused an increase in the k values of cement-treated contaminated samples, probably owing to the aforementioned detrimental impacts of heavy metal on the cement hydrations. This condition can promote the transport of liquids and ions into and from the S/S products and reduce their compatibility against the chemical attack, which agrees well with the TCLP test results. By and large, the results in Fig. 7-b indicate that the introduction of silica fume in the cement matrix contributed to the lower permeability of S/S products. Indeed, the ultra-fine particles of silica fume can act as fillers that may fill the interparticles porosity, resulting in the permeability reduction. The higher decrease in the k values of CSF-treated samples may also be related to greater formation of CSH gel, causing a gradual reduction in the pore-size distribution, and hence, decreasing the soil permeability.

Effects of binders on the microstructural performance of samples

A series of XRD and SEM-EDX experiments were performed to more precisely evaluate the extent of SF contribution on the S/S process and to monitor the changes in microstructure and crystalline phases caused by the treatments. It is shown that the XRD patterns of clays particularly the intensity of major basal spacing peaks can be

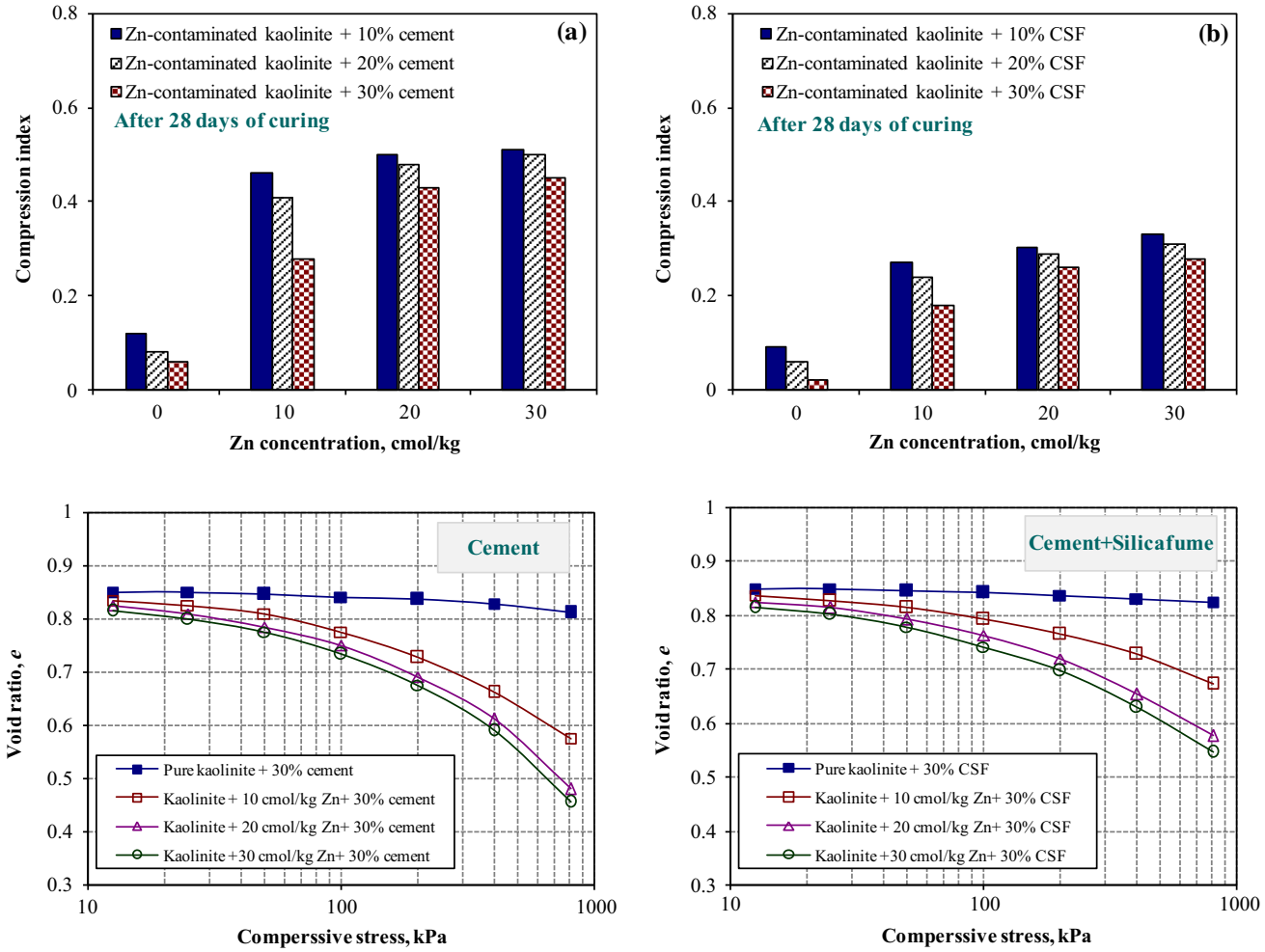

Fig. 6 Variation of the settlement behavior of cement and cement/silica fume (CSF)-treated sample due to interaction with different concentrations of heavy metal

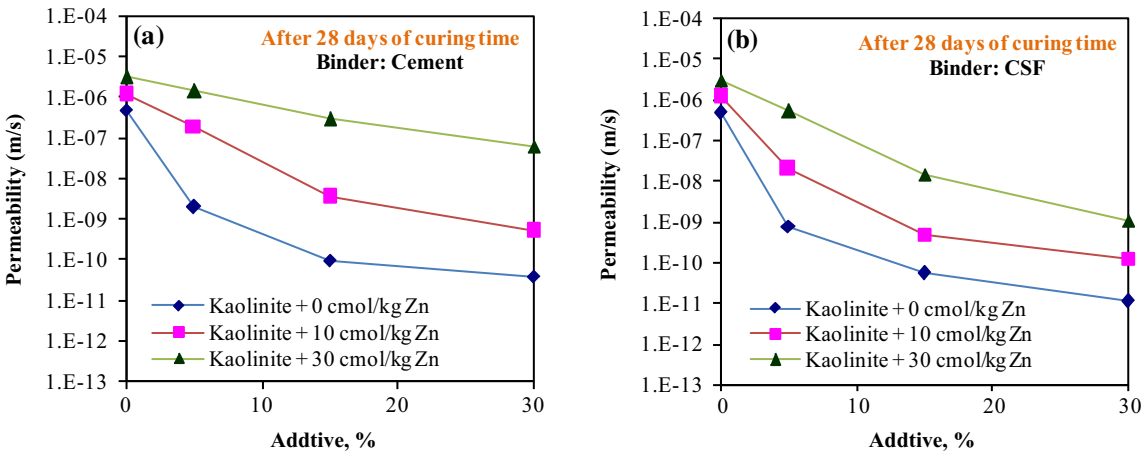

Fig. 7 Effect of Zn concentration and stabilizer addition on the permeability coefficient (k) of treated samples by cement and CSF mixture

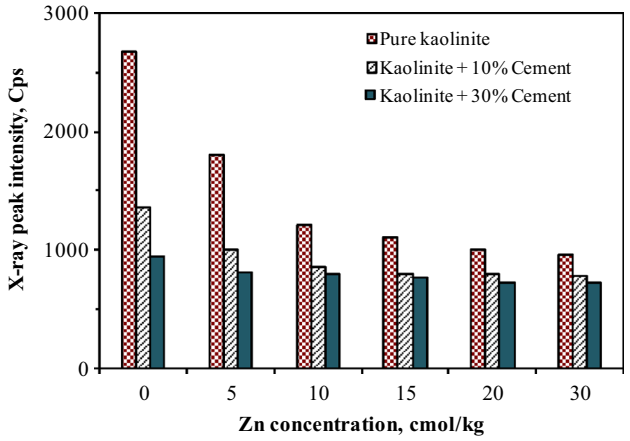

Fig. 8 Effect of Zn concentration and cement dosage on the peak intensity of the major basal spacing of kaolinite soil sample (i.e., $d_{001} = 7.13$ Å)

affected by the nature of pore fluid and stabilizer characteristics (Ouhadi et al. 2014; Goodarzi and Salimi 2015). Therefore, the variations of peak intensity for the major basal spacing of kaolinite (i.e., $d_{001} = 7.13$ Å) upon different concentrations of zinc and cement were determined based on the results of the XRD tests and reported in Fig. 8. As the figure indicates, the peak intensity of untreated samples decreased considerably for an increase in the Zn levels. This is because the clay particles exhibited a much flocculated structure upon contact with HM, as was previously confirmed by the zeta potential value changes (Fig. 3). Those flocculated particles showed lesser peak intensities in response to a decrease in the reflection of incident ray compared with their initial oriented structure. Such a decrease in the clay peak intensity of natural kaolinite with increasing Zn concentration can reduce the interaction of the minerals with HMs and thereby may decrease the soil adsorption capacity. Indeed, according to the diffuse double layer (DDL) theory, the repulsive forces between the clay particles are diminished and the diffuse double layer's thickness is decreased when the pore water is replaced with a liquid of higher electrolyte concentration and/or higher cation valance (e.g., HMs pollutants). Once the DDL shrinks, the soil particles get closer to each other, which could alter the extent of the dispersed structure to a relatively flocculated structure as confirmed by the lower zeta potential (ζ) measured for the Zn-contaminated soil samples. It seems the decrease in ζ can reduce the magnitude of surface potential (ψ) and consequently diminish the charge density and repulsion forces among the negative charged clay surfaces (Kaya and Fang 2005; Goodarzi et al. 2016), leading to flocculation of particles and thereby the reduction in the XRD peak intensity of the clay mineral with increasing the Zn concentration. As a consequence of such microstructural changes, the clay particles become less hydrated and a tighter packing or aggregation of particles (i.e., an increase in the proportion of macro-pores) forms which result in decreasing the heavy metal contaminant adsorption of soil as indicated in Fig. 1. In uncontaminated stabilized soil samples, the kaolinite also appeared to have vanished as the cement content increased. This behavior can be explained by the gradual exhausting of the clay fractions through the pozzolanic reactions, which may enhance the soil mechanical capacity (Ouhadi et al. 2014), as determined from the macro-level experiments. On the other hand, the variations in peak intensity of contaminated soils decreased once the quantity of binder increased, indicating that there was less impact of Zn ions on soil microstructure since most of them were retained at high dosages of agent; hence, due to less interaction of Zn and soil particles, little difference in the peak intensity could be observed. An example of the X-ray patterns for clean and Zn-spiked kaolinite soil with 30 % binder following 28 days of curing is also shown in Fig. 9. As evident from this figure, the decrease in intensities corresponding to the clay mineral's peaks coupled with the presence of some new peaks such as calcium zincate [$CaZn_2(OH)_6 \cdot 2H_2O$] and CSH substantiated the occurrence of microstructural changes in both cement and CSF-treated soils. Based on the variation of CSH peak intensity (the increase in the peak intensity at 2θ about 29°) in Fig. 9d, e, it is obvious that the formation of cementing products decreased considerably for an increase in the Zn concentrations, which in turn demonstrates the retardant effect of heavy metal on the hydration of pozzolanic reactions, as reported by pervious works (Qiao et al. 2007; Chen et al. 2009; Moon et al. 2010; Du et al. 2013). However, at the presence of the same amount of agent, the CSF-treated Zn-contaminated samples showed a more quantity of CSH compound compared with the soil–cement mixtures. For example, the CSH peak intensity in the case of CSF treatment declined to about 28 % with the addition of 30 cmol/kg Zn and to about 52 % in the specimens without SF containing the same amount of pollutant. It is confirmed that a further process of cementing materials formation may have occurred in the CSF-treated samples, which could have lead to a greater strength gain in this case (Fig. 5). The beneficial effects of further CSH gel formation were also observed in the consolidation and TCLP tests, reflecting more enhancement in the soil properties by adding CSF blend as compared to sole cement. In other words, the XRD data provided additional evidence for the above discussion about the enhancing effect of SF on the mechanical properties of the composite cementing system and its durability. As shown in Fig. 9, the incorporation of SF into the cement caused acceleration rather than retardation of HM on the cementitious products formation, because of the large amount of silica present in SF, which

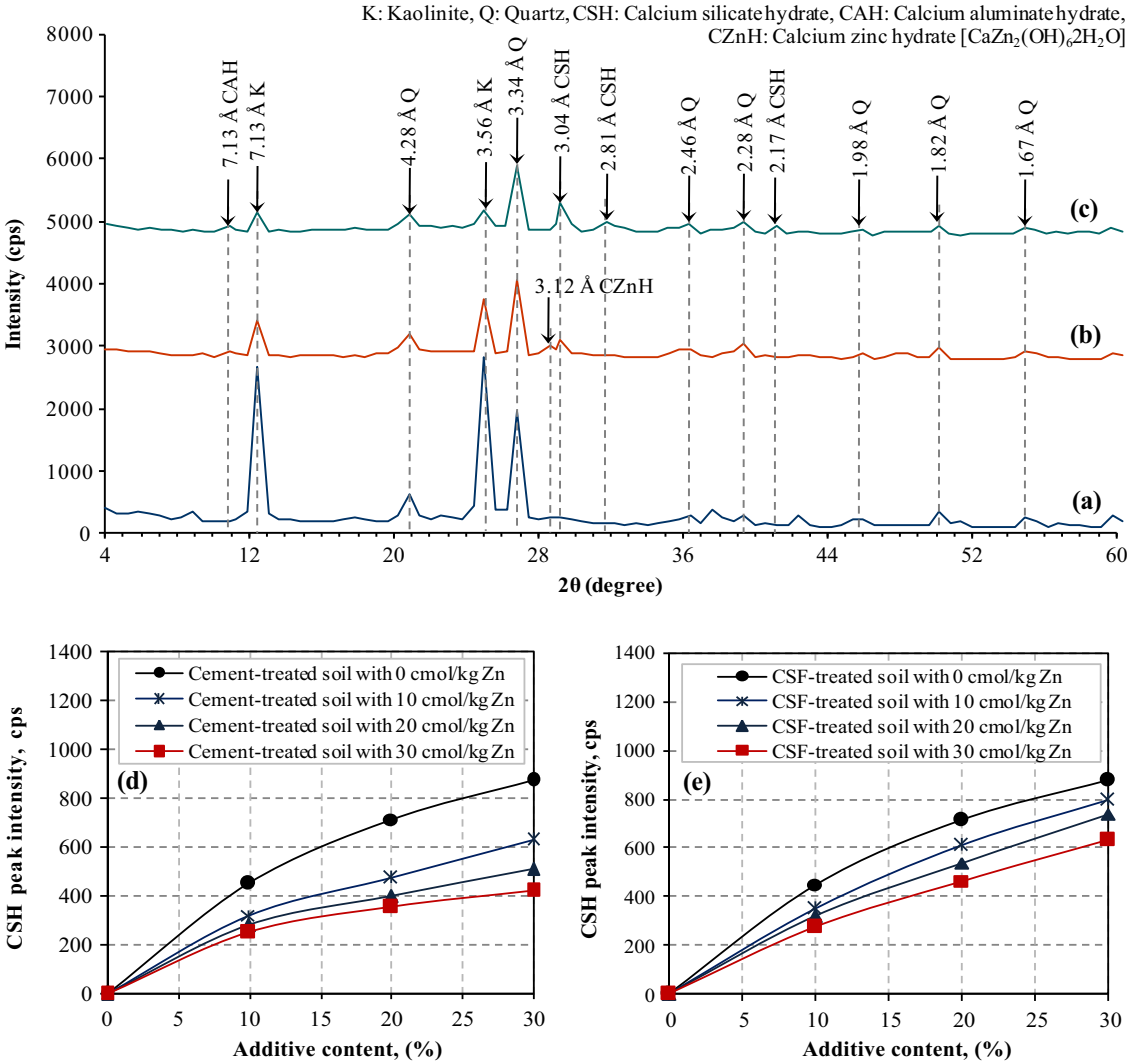

Fig. 9 XRD analysis; **a** natural kaolinite, **b** contaminated kaolinite with 30 cmol/kg Zn + 30 % cement after 28 days of curing, **c** contaminated kaolinite with 30 cmol/kg Zn + 30 % CSF after 28 days of curing, **d** CSH peak intensity variation of Zn-contaminated soil treated with cement and **e** CSH peak intensity variation of Zn-contaminated soil treated with CSF

may have caused the formation of additional calcium silica hydrate (CSH) bonding between the silica and the free lime liberated during cement hydration. Once the calcium hydroxide, which is a weak part in hydration product, was consumed for the secondary CSH gel formation, more linkages of solid phase could be formed, allowing to improve both the mixture particle packing and the compactness of S/S product (see SEM micrographs in Fig. 10); therefore, an increase in the compressive strength of the contaminated soil containing composite cement-SF and a decrease in its settlement occurred. Besides, it has been reported that Zn ions can directly be incorporated into calcium silica hydrate compounds. The zinc substitution occurs either by replacement of calcium ions or by direct linkage to the end of the silicate chains through Zn–O–Si bonds, leading to a decrease in the CSH content (Moulin et al. 1999; Rose et al. 2001; Moon et al. 2010). Thus, based on such microstructural changes and with respect to the enhancing effect of silica fume on the pozzolanic reactions which promote the hydration process, the additional cementing phases were identified in the XRD patterns of CSF treatment as compared with cement-stabilized contaminated soils. In addition, the development of calcium zincate as evidence for the retardation of cement hydration (Qiao et al. 2007; Du et al. 2014b) was mainly detected upon the cement treatment (Fig. 9b), but it could not be identified when silica fume was added to the system (Fig. 9c). The absence of calcium zincate in the CSF-treated soils, which has an opposite trend as compared to that of CSH gel formation in those samples, could be explained by the pozzolanic interactions of SF with cement, a process during which Ca^{2+} ions are consumed

and the chemical reactions between portlandite and Zn are reduced. This results in a decrease in the calcium zincate intensity and promotes the cement hydration process, indicating that solidification condition can be facilitated upon CSF treatment, as was shown by the macro-level tests. It should be noted that the formation of calcium zincate can particularly retard the early hydration of tri-calcium silicate (C_3S) because this precipitate covers cement grains and prevents the material transport, which is necessary for their hydration to continue (Chen et al. 2009; Du et al. 2014b; Wang et al. 2015b). Accordingly, the cement-stabilized samples exhibit porous structures as compared to that in CSF treatment, which is substantiated by the SEM images (Fig. 10b, c).

Figure 10 shows the SEM micrographs of clean soil (Fig. 10a), Zn-contaminated soil with 30 % cement (Fig. 10b) and Zn-contaminated soil with 30 % CSF (Fig. 10c) cured for 28 days. The microstructure of the stabilized soils is quite different as compared to the natural kaolinite. Figure 10-b demonstrates the flocculated nature of the fabric and the formation of new cementing compounds in the matrix of the cement-stabilized sample. The flocculated structure could be associated with the cation-exchange process, resulting in replacement of calcium ions liberated during cement hydration with readily exchangeable ions such as Na^+ ions (Shen et al. 2008; Du et al. 2013). However, the flocculated condition is almost invisible and a large quantity of cementitious matter is

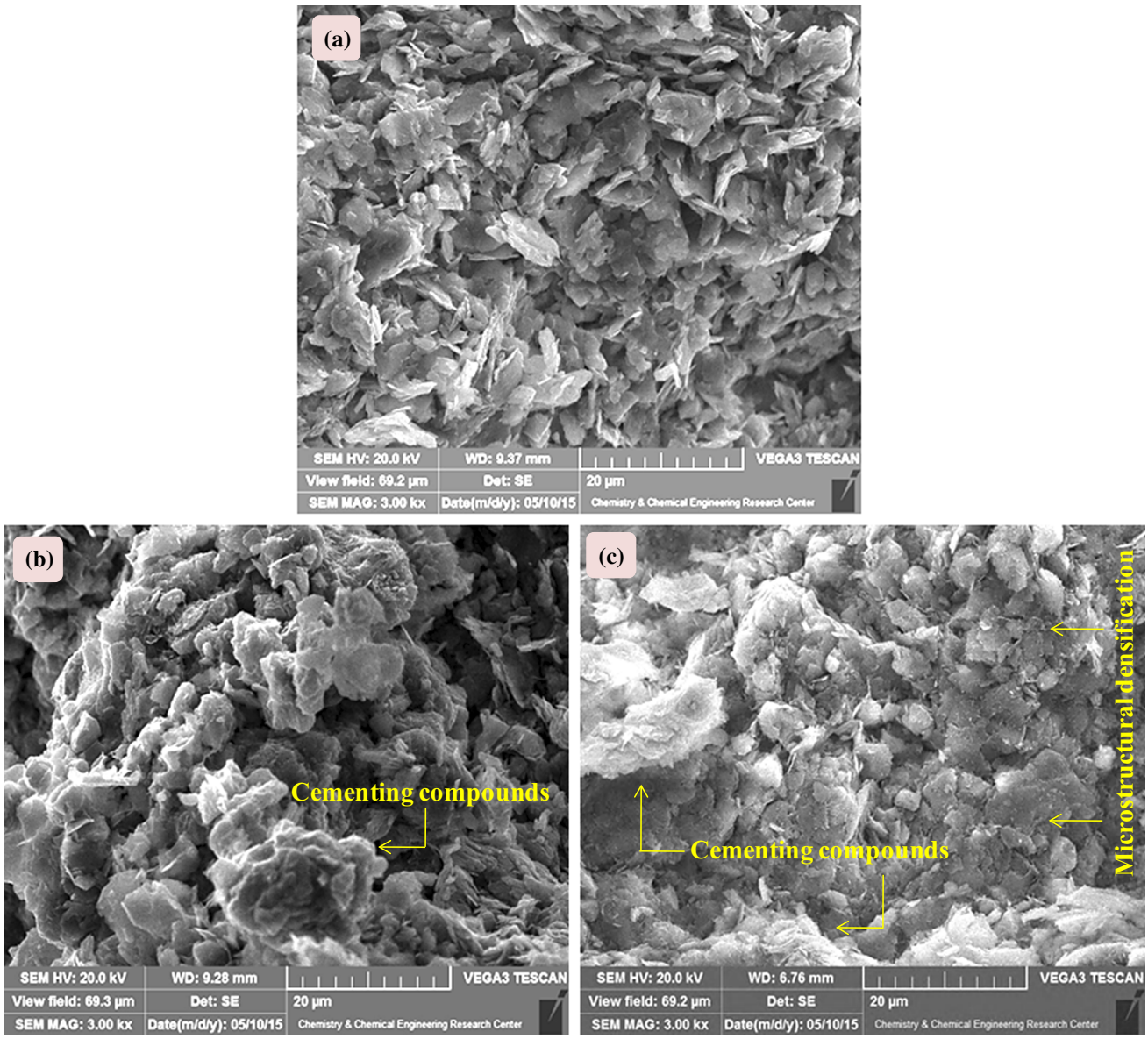

Fig. 10 SEM micrographs; **a** natural kaolinite, **b** contaminated kaolinite with 30 cmol/kg Zn + 30 % cement cured for 28 days, **c** contaminated kaolinite with 30 cmol/kg Zn + 30 % CSF cured for 28 days

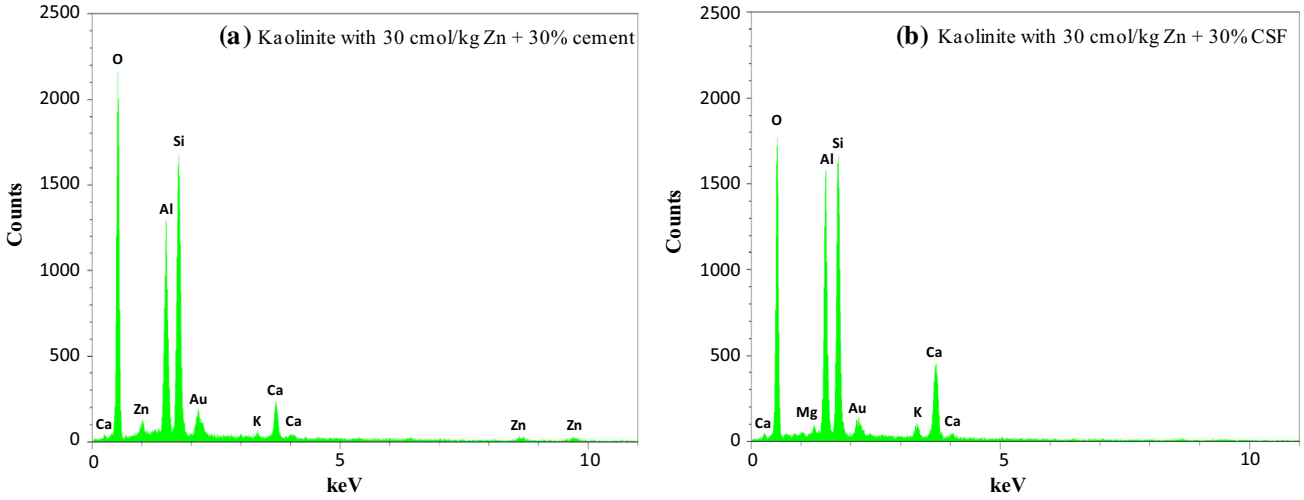

Fig. 11 EDX spectrums of Zn-contaminated kaolinite under cement and cement/silica fume (CSF) treatment after 28 days of curing

formed upon CSF treatment as a result of the pozzolanic interactions of SF with cement, a process which is confirmed by the XRD analysis mentioned above (see Fig. 9) and consumes Ca^{2+} ions and produces additional CSH. Based on the SEM micrographs, the addition of binder generally transforms the soil fabric from a particle-based form to an integrated composition. This phenomenon was more prominently observed upon CSF treatment; however, great many pores are presented in treated soil sample without SF, indicating that the cementing products have not been fully developed, the surface of soil particles has not been completely covered, and the pores of soil have not been fully filled by the hydration gels. Also, the existence of more plate-shaped crystals of hydroxide calcium can be detected in the cement-treated samples. These show that the formation of cementitious compounds has not yet occurred completely, which further confirms that the presence of heavy metal ions can delay the conduction of the hydration process. However, the cementing products are less fragmentized and some small pores can be seen in the matrices having cement + SF. In such case, a large amount of the hydration gel forms, which covers the surface of the clay particles and expands in the pores of soil. The mechanism behind this is connected not only to chemical formation of additional CSH bonding between the silica and the free lime (i.e., pozzolanic reaction) at the interface, but also to the microstructure modification (i.e., calcium hydroxide orientation, porosity and transition zone thickness) as addressed before. Furthermore, the extreme fineness of SF particles could make them very efficient fillers which result in a reduced volume of larger soil pores and serve to distribute the new crystalline phases in a more homogenous fashion in the available space, leading to pore-size refinement and matrix densification which exhibit good fixation efficiency of heavy metal (see Fig. 4). In addition to the XRD tests, the EDX analyses were used as secondary evidence of mineral identification, as suggested by previous works (Moon et al. 2009, 2010; Fernández-Carrasco et al. 2014; Muller et al. 2015; Wang et al. 2015b; Maheswaran et al. 2016). The EDX results (Fig. 11a, b) revealed that the Ca:Si ratio upon CSF application was around 30 %, whereas this ratio was somewhat higher at 14 % for samples with the sole cement. The further increase in the Ca:Si ratio can be explained due to more CSH gel formation (Eisazadeh et al. 2012), which is highly consistent with the final leachate pH observations in Fig. 4, because as was previously discussed, the relatively lower pH circumstance in the case of CSF treatment may imply that more pozzolanic reactions occurred with the incorporation of silica fume into the cement matrix, depositing higher CSH gel on the surface of the particles, which increased the Ca:Si ratio. The EDX spectrums also showed that the Zn content would have a relatively higher value in the cement-treated sample compared with the CSF application. This is consistent with the mechanism by which the more calcium zincate is produced and settled on the surface of soil particles at the presence of sole cement, as was clearly illustrated by the XRD patterns. In other words, comparison of Fig. 11a, b illustrates that no Ca-Zn^{2+} compounds were identified in CSF-stabilized sample, indicating that no retardation occurred during CSF treatment. This suggests that the micro- and/or macro-encapsulations which are the results of a higher pozzolanic activity and matrix densification are the main parameters controlling HM leachability in the CSF-treated soils. Finally, the beneficial impacts of the observed higher formation of cementing compounds and lower deleterious reactions between Zn and cement products under the CSF

treatment were clearly seen (see Figs. 5, 6, 7) to have enhanced the geo-mechanical properties of S/S materials.

Conclusions

- The results obtained reveal that the adsorption capability of the natural kaolinite decreases as the zinc concentration increases. This is attributed to the reduction in the surface charge density of the clay particles and development of aggregated structure, as is clearly confirmed by decreasing the absolute value of zeta potential and diminishing the XRD peak intensity of the clay mineral upon contact with the heavy metal (HM) pollutant.
- The application of low cement dosage ($\approx$10 %) considerably enhances the HM retention capacity of kaolinite by raising the pH level; however, this may be partly lost, and hence, the HM is released when the soil–cement system is acidified. As a result, high percentage (>30 %) of binder should be employed to meet the full needs of HM immobilization in the heavily zinc ($\approx$30 cmol/kg Zn)-contaminated soil. The strength and compressibility of cement-treated samples are also adversely affected by increasing zinc concentration. Such a behavior, as determined by the micro-level tests, is due to the deleterious impact of Zn on the gel formation step of cement hydration, resulting in the degradation of soil particles interlocking.
- It appears that incorporation of silica fume (SF) into the binder system causes a reduction in the detrimental effects of aggressive environment and HM on the performance of cement-based S/S products. In this case, the samples amended with the CSF blend exhibit an increase in the strength up to 50 % compared with the stabilized soils with sole cement. The CSF-treated samples also attain a lower HM leachability and are less deformable as they show a decrease in their compression index by nearly 40 %.
- Based on the XRD and SEM-EDX analyses, the superior influences of CSF are mainly ascribed to the higher and faster formation of cementitious compounds. Moreover, SF reduces the pores sizes and serves to distribute the new crystalline phases in a more homogenous fashion in the available space. This microstructural reorganization upon the CSF treatment provides higher environmentally stable materials with lower cost and energy as compared to stand-alone cement.
- From a practical point of view, an optimum CSF content of 1 wt% per 1 cmol/kg of HM within 7 days of curing can satisfy the EPA-accepted criteria of the TCLP and UCS values and, therefore, is recommended to successfully remediate the zinc-contaminated soils.

References

Abo-El-Enein SA, El-kady G, El-Sokkary TM, Gharieb M (2015) Physico-mechanical properties of composite cement pastes containing silica fume and fly ash. HBRC J 11:7–15

Antemir A, Hills CD, Carey PJ, Gardner KH, Bates ER, Crumbie AK (2010) Long-term performance of aged waste forms treated by stabilization/solidification. J Hazard Mater 181:65–73

Asavapisit S, Nanthamontry W, Polprasert C (2001) Influence of condensed silica fume on the properties of cement-based solidified wastes. Cem Concr Res 31:1147–1152

ASTM (2006) Annual book of ASTM standards, vol 04.08. American Society for Testing and Materials, Philadelphia

Benaicha M, Roguiez X, Jalbaud O, Burtschell Y, Alaoui AH (2015) Influence of silica fume and viscosity modifying agent on the mechanical and rheological behavior of self compacting concrete. Constr Build Mater 84:103–110

Chauhan RP, Kumar A (2013) Study of radon transport through concrete modified with silica fume. Radiat Meas 59:59–65

Chemeda YC, Deneele D, Christidis GE, Ouvrard G (2015) Influence of hydrated lime on the surface properties and interaction of kaolinite particles. Appl Clay Sci 107:1–13

Chen QY, Tyrer M, Hills CD, Yang XM, Carey P (2009) Immobilisation of heavy metal in cement-based solidification/stabilisation: a review. Waste Manag 29:390–403

Chiang PN, Tong OY, Chiou CS, Lin YA, Wang MK, Liu CC (2016) Reclamation of zinc-contaminated soil using a dissolved organic carbon solution prepared using liquid fertilizer from food-waste composting. J Hazard Mater 301:100–105

Choi WH, Lee SR, Park JY (2009) Cement based solidification/stabilization of arsenic-contaminated mine tailings. Waste Manag 29:1766–1771

Çoruh S, Elevli S, Ergun ON, Demir G (2013) Assessment of leaching characteristics of heavy metals from industrial leach waste. Int J Miner Process 123:165–171

Coz A, Andrés A, Soriano S, Viguri JR, Ruiz MC, Irabien JA (2009) Influence of commercial and residual sorbents and silicates as additives on the stabilisation/solidification of organic and inorganic industrial waste. J Hazard Mater 164:755–761

Cuisinier O, Borgne TL, Deneele D, Masrouri F (2011) Quantification of the effects of nitrates, phosphates and chlorides on soil stabilization. Eng Geol 117:229–235

Dmuchowski W, Gozdowski D, Brągoszewska P, Baczewska AH, Suwara I (2014) Phytoremediation of zinc contaminated soils using silver birch (*Betula pendula* Roth). Ecol Eng 71:32–35

Du YJ, Jiang NJ, Liu SY, Jin F, Singh DN, Puppala AJ (2013) Engineering properties and microstructural characteristics of cement-stabilized zinc-contaminated kaolin. Can Geotech J 51:289–302

Du YJ, Wei ML, Reddy KR, Jin F (2014a) Compressibility of cement-stabilized zinc-contaminated high plasticity clay. Nat Hazards 73:671–683

Du YJ, Wei ML, Reddy KR, Jin F, Wu HL, Liu ZB (2014b) New phosphate-based binder for stabilization of soils contaminated with heavy metals: leaching, strength and microstructure characterization. J Environ Manage 146:179–188

Du YJ, Wei ML, Reddy KR, Wu HL (2016) Effect of carbonation on leachability, strength and microstructural characteristics of KMP

binder stabilized Zn and Pb contaminated soils. Chemosphere 144:1033–1042
Eisazadeh A, Kassim KA, Nur H (2012) Stabilization of tropical kaolin soil with phosphoric acid and lime. Nat Hazards 61(931–942):2012
Elaty MAA, Ghazy MF (2014) Performance of Portland cement mixes containing silica fume and mixed with lime-water. HBRC J 10:247–257
El-Eswed BI, Yousef RI, Alshaaer M, Hamadneh I, Al-Gharabli SI, Khalili F (2015) Stabilization/solidification of heavy metals in kaolin/zeolite based geopolymers. Int J Miner Process 137:34–42
EPA (1983) Process design manual: land application of municipal sludge, Res. Lab. EPA-625/1-83-016
Erdem M, Özverdi A (2011) Environmental risk assessment and stabilization/solidification of zinc extraction residue: II. Stabilization/solidification. Hydrometallurgy 105:270–276
Fernández-Carrasco L, Claramunt J, Ardanuy M (2014) Autoclaved cellulose fiber reinforced cement: effects of silica fume. Constr Build Mater 66:138–145
Goodarzi AR, Akbari HR (2014) Assessing the anion type effect on the hydro-mechanical properties of smectite from macro and micro-structure aspects. Geomech Eng 7:183–200
Goodarzi AR, Salimi M (2015) Stabilization treatment of a dispersive clayey soil using granulated blast furnace slag and basic oxygen furnace slag. Appl Clay Sci 108:61–69
Goodarzi AR, Fateh SN, Shekary H (2016) Impact of organic pollutants on the macro and microstructure responses of Na-bentonite. Appl Clay Sci 121:17–28
Hekal EE, Hegazi WS, Kishar EA, Mohamed MR (2011) Solidification/stabilization of Ni(II) by various cement pastes. Constr Build Mater 25:109–114
Hot J, Cyr M, Augeard E, Eekhout M (2015) An investigation of CaSi silica fume characteristics and its possible utilization in cement-based and alkali-activated materials. Constr Build Mater 101:456–465
Hunter RJ (2013) Zeta potential in colloid science: principles and applications, vol 2. Academic press, New York
Jalal M, Pouladkhan A, Harandi OF, Jafari D (2015) Comparative study on effects of Class F fly ash, nano silica and silica fume on properties of high performance self compacting concrete. Constr Build Mater 94:90–104
John UE, Jefferson I, Boardman DI, Ghataora GS, Hills CD (2011) Leaching evaluation of cement stabilisation/solidification treated kaolin clay. Eng Geol 123:315–323
Jun KS, Hwang BG, Shin HS, Won YS (2001) Chemical characteristics and leachability of organically contaminated heavy metal sludge solidified by silica fume and cement. Water Sci Technol 44:399–407
Kalkan E (2011) Impact of wetting-drying cycles on swelling behavior of clayey soils modified by silica fume. Appl Clay Sci 52:345–352
Kalkan E (2013) Preparation of scrap tire rubber fiber–silica fume mixtures for modification of clayey soils. Appl Clay Sci 80:117–125
Kang Y, Jeong SG, Wi S, Kim S (2015) Energy efficient Bio-based PCM with silica fume composites to apply in concrete for energy saving in buildings. Sol Energy Mater Sol Cells 143:430–434
Kaya A, Fang HY (2000) The effects of organic fluids on physicochemical parameters of fine-grained soils. Can Geotech J 37:943–950
Kaya A, Fang HY (2005) Experimental evidence of reduction in attractive and repulsive forces between clay particles permeated with organic liquids. Can Geotech J 42:632–640
Kaya A, Yukselen Y (2005) Zeta potential of soils with surfactants and its relevance to electrokinetic remediation. J Hazard Mater 120:119–126
Ko TH, Shih MH, Hsueh HT (2007) Spectroscopic study on the zinc-contaminated soils for the determination of zinc speciation.Spectrochimica Acta Part A. Mol Biomol Spectrosc 66:442–447
Kogbara RB, Al-Tabbaa A, Yi Y, Stegemann JA (2013) Cement–fly ash stabilisation/solidification of contaminated soil: performance properties and initiation of operating envelopes. Appl Geochem 33:64–75
Koksal F, Gencel O, Kaya M (2015) Combined effect of silica fume and expanded vermiculite on properties of lightweight mortars at ambient and elevated temperatures. Constr Build Mater 88:175–187
Koteng DO, Chen CT (2015) Strength development of lime–pozzolana pastes with silica fume and fly ash. Constr Build Mater 84:294–300
Kumpiene J, Lagerkvist A, Maurice C (2008) Stabilization of As, Cr, Cu, Pb and Zn in soil using amendments–a review. Waste Manag 28:215–225
Lemaire K, Deneele D, Bonnet S, Legret M (2013) Effects of lime and cement treatment on the physicochemical, microstructural and mechanical characteristics of a plastic silt. Eng Geol 166:255–261
Li X, Chen Q, Zhou Y, Tyrer M, Yu Y (2014) Stabilization of heavy metals in MSWI fly ash using silica fume. Waste Manag 34:2494–2504
Li JS, Xue Q, Wang P, Li Z (2015) Effect of lead (II) on the mechanical behavior and microstructure development of a Chinese clay. Appl Clay Sci 105–106:192–199
Liu J, Li Y, Ouyang P, Yang Y (2015) Hydration of the silica fume-Portland cement binary system at lower temperature. Constr Build Mater 93:919–925
Maheswaran S, Kalaiselvam S, Karthikeyan SS, Kokila C, Palani GS (2016) β-Belite cements (β-dicalcium silicate) obtained from calcined lime sludge and silica fume. Cement Concr Compos 66:57–65
Malamis S, Katsou E (2013) A review on zinc and nickel adsorption on natural and modified zeolite, bentonite and vermiculite: examination of process parameters, kinetics and isotherms. J Hazard Mater 252:428–461
Malviya R, Chaudhary R (2006) Factors affecting hazardous waste solidification/stabilization: a review. J Hazard Mater 137:267–276
Moon DH, Grubb DG, Reilly TL (2009) Stabilization/solidification of selenium-impacted soils using Portland cement and cement kiln dust. J Hazard Mater 168:944–951
Moon DH, Lee JR, Grubb DG, Park JH (2010) An assessment of Portland cement, cement kiln dust and Class C fly ash for the immobilization of Zn in contaminated soils. Environ Earth Sci 61:1745–1750
Moulin I, Stone WEE, Sanz J, Bottero JY, Mosnier F, Haehnel C (1999) Lead and zinc retention during hydration of tri-calcium silicate: a study by sorption isotherms and 29Si nuclear magnetic resonance spectroscopy. Langmuir 15:2829–2835
Muller ACA, Scrivener KL, Skibsted J, Gajewicz AM, McDonald PJ (2015) Influence of silica fume on the microstructure of cement pastes: new insights from ^{1H}NMR relaxometry. Cem Concr Res 74:116–125
Nazari A, Riahi S (2011) The effects of SiO_2 nanoparticles on physical and mechanical properties of high strength compacting concrete. Compos B 42:570–578
Nili M, Ehsani A (2015) Investigating the effect of the cement paste and transition zone on strength development of concrete containing nanosilica and silica fume. Mater Des 75:174–183
Ouhadi VR, Yong RN, Sedighi M (2006) Desorption response and degradation of buffering capability of bentonite, subjected to heavy metal contaminants. Eng Geol 85:102–110
Ouhadi VR, Yong RN, Shariatmadari N, Saeidijam S, Goodarzi AR, Safari-Zanjani M (2010) Impact of carbonate on the efficiency of

heavy metal removal from kaolinite soil by the electrokinetic soil remediation method. J Hazard Mater 173:87–94

Ouhadi VR, Yong RN, Amiri M, Ouhadi MH (2014) Pozzolanic consolidation of stabilized soft clays. Appl Clay Sci 95:111–118

Qiao XC, Poon CS, Cheeseman CR (2007) Investigation into the stabilization/solidification performance of Portland cement through cement clinker phases. J Hazard Mater 139:238–243

Rose J, Moulin I, Mason A, Bertsch PM, Wiesner MR, Bottero JY, Mosnier F, Haehnel C (2001) X-ray absorption spectroscopy study of immobilization processes for heavy metals in calcium silicate hydrates. 2. Zinc Langmuir 17:3658–3665

Ruiz MC, Irabien A (2004) Environmental behavior of cement-based stabilized foundry sludge products incorporating additives. J Hazard Mater 109:45–52

Saeed KH, Kassim KA, Nur H, Yunus NZM (2015) Strength of lime-cement stabilized tropical lateritic clay contaminated by heavy metals. KSCE J Civil Eng 19:887–892

Sanjuán MÁ, Argiz C, Gálvez JC, Moragues A (2015) Effect of silica fume fineness on the improvement of Portland cement strength performance. Constr Build Mater 96:55–64

Saraya MESI (2014) Study physico-chemical properties of blended cements containing fixed amount of silica fume, blast furnace slag, basalt and limestone, a comparative study. Constr Build Mater 72:104–112

Shen SL, Han J, Du YJ (2008) Deep mixing induced property changes in surrounding sensitive marine clays. J Geotech Geoenviron Eng 134:845–854

Shen Z, Som AM, Wang F, Jin F, McMillan O, Al-Tabbaa A (2016) Long-term impact of biochar on the immobilisation of nickel (II) and zinc (II) and the revegetation of a contaminated site. Sci Total Environ 542:771–776

Soares MA, Quina MJ, Quinta-Ferreira RM (2015) Immobilisation of lead and zinc in contaminated soil using compost derived from industrial eggshell. J Environ Manage 164:137–145

Stephan CH, Courchesne F, Hendershot WH, McGrath SP, Chaudri AM, Sappin-Didier V, Sauvé S (2008) Speciation of zinc in contaminated soils. Environ Pollut 155:208–216

Tantawy MA, El-Roudi AM, Salem AA (2012) Immobilization of Cr(VI) in bagasse ash blended cement pastes. Constr Build Mater 30:218–223

Tsai CH, Huang R, Lin WT, Wang HN (2014) Mechanical and cementitious characteristics of ground granulated blast furnace slag and basic oxygen furnace slag blended mortar. Mater Des 60:267–273

Voglar GE, Lestan D (2013) Equilibrium leaching of toxic elements from cement stabilized soil. J Hazard Mater 246–247:18–25

Voglar GE, Leštan D (2010) Solidification/stabilisation of metals contaminated industrial soil from former Zn smelter in Celje, Slovenia, using cement as a hydraulic binder. J Hazard Mater 178:926–933

Wang F, Wang H, Jin F, Al-Tabbaa A (2015a) The performance of blended conventional and novel binders in the in situ stabilisation/solidification of a contaminated site soil. J Hazard Mater 285:46–52

Wang L, Tsang DCW, Poon CS (2015b) Green remediation and recycling of contaminated sediment by waste-incorporated stabilization/solidification. Chemosphere 122:257–264

Wei ML, Du YJ, Jiang NJ (2012) Compression behavior of zinc contaminated clayey soils solidified with cement. In: Proceedings of GeoCongress 2012: state of the art and practice in geotechnical engineering, Oakland, Calif., 25–25 March 2012. American Society of Civil Engineers, New York, pp 4042–4049

Xi Y, Wu X, Xiong H (2014) Solidification/stabilization of Pb-contaminated soils with cement and other additives. Soil Sediment Contam Int J 23:887–898

Yan J, Quan G, Ding C (2013) Effects of the combined pollution of lead and cadmium on soil urease activity and nitrification. Procedia Environ Sci 18:78–83

Yong RN, Ouhadi VR, Goodarzi AR (2009) Effect of Cu^{2+} ions and buffering capacity on smectite microstructure and performance. J Geotech Geoenviron Eng 135:1981–1985

Zha FS, Liu JJ, Xu L, Cui KR (2013) Effect of cyclic drying and wetting on engineering properties of heavy metal contaminated soils solidified/stabilized with fly ash. J Cent South Univ 20:1947–1952

Zhang Z, Guo G, Teng Y, Wang J, Rhee JS, Wang S, Li F (2015) Screening and assessment of solidification/stabilization amendments suitable for soils of lead-acid battery contaminated site. J Hazard Mater 288:140–146

Zhang Z, Zhang B, Yan P (2016) Comparative study of effect of raw and densified silica fume in the paste, mortar and concrete. Constr Build Mater 105:82–93

Zhou Y, Yao J, Choi MM, Chen Y, Chen H, Mohammad R, Zhuang R, Chen H, Wang F, Maskow T, Zaray G (2009) A combination method to study microbial communities and activities in zinc contaminated soil. J Hazard Mater 169:875–881